OXFORD

*Human Molecular Genetics*, 2015, Vol. 24, No. 9 2539–2551

**doi: 10.1093/hmg/ddv018**
Advance Access Publication Date: 23 January 2015
Original Article

ORIGINAL ARTICLE

# miRNA-558 promotes tumorigenesis and aggressiveness of neuroblastoma cells through activating the transcription of heparanase

Hongxia Qu[1,†], Liduan Zheng[2,3,†], Jiarui Pu[1,†], Hong Mei[1], Xuan Xiang[1], Xiang Zhao[1], Dan Li[1], Shiwang Li[1], Ling Mao[4], Kai Huang[3] and Qiangsong Tong[1,3,*]

[1]Department of Pediatric Surgery, [2]Department of Pathology, [3]Clinical Center of Human Genomic Research and [4]Department of Neurology, Union Hospital, Tongji Medical College, Huazhong University of Science and Technology, Wuhan, Hubei Province 430022, People's Republic of China

*To whom correspondence should be addressed at: Department of Pediatric Surgery, Union Hospital, Tongji Medical College, Huazhong University of Science and Technology, Wuhan 430022, Hubei Province, People's Republic of China. Tel: +86 2785726005; Fax: +86 2785726821; Email: qs_tong@hotmail.com

## Abstract

Heparanase (HPSE) is the endogenous endoglycosidase that degrades heparan sulfate proteoglycans and promotes the tumor growth, invasion, metastasis and angiogenesis. Our previous studies have shown that HPSE is highly expressed in neuroblastoma (NB), the most common extracranial solid tumor in childhood. However, the underlying regulatory mechanisms remain largely unknown. In this study, we identified one binding site of microRNA-558 (miR-558) within the *HPSE* promoter. In NB tissues and cell lines, miR-558 was up-regulated and positively correlated with HPSE expression. Gain- and loss-of-function studies demonstrated that miR-558 facilitated the transcript and protein levels of HPSE and its downstream gene, vascular endothelial growth factor, in NB cell lines. In addition, miR-558 enhanced the promoter activities of *HPSE*, and these effects were abolished by the mutation of the miR-558-binding site. Mechanistically, miR-558 induced the enrichment of the active epigenetic marker and RNA polymerase II on the *HPSE* promoter in NB cells in an Argonaute 1-dependent manner, which was abolished by repressing the miR-558-promoter interaction. Knockdown of endogenous miR-558 decreased the growth, invasion, metastasis and angiogenesis of NB cells *in vitro* and *in vivo*. In contrast, over-expression of miR-558 promoted the growth, invasion, metastasis and angiogenesis of SH-SY5Y and SK-N-SH cells. Restoration of HPSE expression prevented the NB cells from changes in these biological features induced by knockdown or over-expression of miR-558. These data indicate that miR-558 induces the transcriptional activation of *HPSE* via the binding site within promoter, thus facilitating the tumorigenesis and aggressiveness of NB.

## Introduction

Neuroblastoma (NB), the most common extracranial solid tumor derived from the neural crest, is characterized by heterogeneous biological behaviors, ranging from spontaneous regression to aggressive progression, and accounts for almost 15% of all childhood cancer deaths (1). For high-risk NB patients, invasion and metastasis are the leading causes of death, which remains a major therapeutic challenge in pediatric oncology (1). Better elucidating the mechanisms underlying the tumorigenesis and aggressiveness of NB is needed for improving the therapeutic efficiency. Heparanase (HPSE) is the only endogenous endoglycosidase that degrades the heparan sulfate proteoglycans in the

[†]H.Q., L.Z. and J.P. contributed equally to this work.

**Received:** October 25, 2014. **Revised:** January 6, 2015. **Accepted:** January 19, 2015

© The Author 2015. Published by Oxford University Press. All rights reserved. For Permissions, please email: journals.permissions@oup.com

extracellular matrix and the basement membrane, enabling tumor cells to break through these barriers for invasion and metastasis (2). In addition, HPSE regulates tumor growth and angiogenesis through releasing multiple types of cytokine and promoting the formation of new vessels (3). Recent evidence shows that apart from its enzymatic activity, HPSE is able to increase the transcriptional and protein levels of vascular endothelial growth factor (VEGF) in breast cancer and glioma cells via the activation of Src family members (4), further supporting a pro-angiogenic function of HPSE in tumor progression. A series of studies have demonstrated that HPSE expression is elevated in colorectal cancer (5), pancreatic cancer (6), bladder cancer (7), gastric cancer (8) and cervical cancer (9) and is associated with aggressive phenotypes and poor prognosis (3). In our previous studies, we have found that HPSE is up-regulated in NB tissues (10), and knockdown of *HPSE* attenuates the growth and aggressiveness of human cancer cells (11,12). However, the regulatory mechanisms underlying the HPSE expression in NB still remain largely unknown.

MicroRNAs (miRNAs), a class of endogenous non-coding RNAs containing 20–25 nucleotides, are involved in gene expression regulation through targeting their binding sites, usually in the 3′-untranslated region (3′-UTR) of mRNA, and lead to post-transcriptional or translational repression (13). Evidence shows that miRNAs play potent oncogenic or tumor suppressive roles in many cellular processes, including proliferation, apoptosis, invasion and metastasis (13). Canonically, these processes are executed through the recognition of miRNA–mRNA interaction by RNA-induced silencing complex machinery, with Argonaute (AGO) proteins as the main effector (14,15). Previous studies have shown that miR-1258 inhibits the expression of HPSE through targeting its 3′-UTR, resulting in decreased brain metastasis of breast cancer cells (16). In recent years, emerging studies reveal that certain miRNAs regulate gene expression at the transcriptional levels in human cells (17–20). However, the roles of miRNAs in regulating the transcription of *HPSE* still remain unclear. In the current study, we demonstrate, for the first time, that miroRNA-558 (miR-558) is up-regulated and positively correlated with HPSE expression in NB tissues and cell lines and directly targets the *HPSE* promoter to activate its transcription, thus promoting the growth, invasion, metastasis and angiogenesis of NB cells *in vitro* and *in vivo*, suggesting the crucial roles of miR-558 in the progression and aggressiveness of NB.

## Results

### miR-558 was up-regulated and positively correlated with HPSE levels in NB tissues and cell lines

Our previous studies have initially revealed the high expression of HPSE in primary NB tissues (10). To investigate the hypothesis that miRNA may regulate the transcription of *HPSE* in NB, computational prediction was performed by the miRNA–promoter interaction database (21) and AGO–chromosome interaction profiling data (GSE40536). Enrichment of AGO1, but not of AGO2, was noted at bases −2468/−2591 upstream the transcription start site (TSS) of *HPSE*. Surrounding this region, there were potential binding sites of miR-145, miR-558 and miR-17 with high complementarity, locating at bases −2330/−2345, −2314/−2332 and −2292/−2313 relative to the *HPSE* TSS (Fig. 1A). The dual-luciferase assay indicated that the transfection of the miRNA inhibitor and the mimic of miR-558, but not of miR-145 or miR-17, resulted in altered promoter activities of *HPSE* in cultured NB cell lines (Fig. 1A). Mining the publicly available clinical tumor expression data sets [R2: microarray analysis and visualization platform (http://r2.amc.nl)] revealed that the expression of baculoviral IAP repeat containing 6 (BIRC6), the host gene of miR-558 (22), was up-regulated in specimens from 88 well-established NB cases than that in normal dorsal ganglia ($P < 0.0001$, Supplementary Material, Fig. S1A). In addition, the BIRC6 levels were correlated with advanced international NB staging system (INSS) stages ($P = 0.007$, Supplementary Material, Fig. S1A) and aggressiveness of neuroblastic tumors ($P = 0.0079$, Supplementary Material, Fig. S1B). There was a positive correlation between *BIRC6* and *MYCN* transcript levels in NB tissues (correlation coefficient $R = 0.346$, $P = 9.7 \times 10^{-4}$, Supplementary Material, Fig. S1C) or neuroblastic tumors ($R = 0.497$, $P = 2.9 \times 10^{-5}$, Supplementary Material, Fig. S1C). Higher BIRC6 expression was also observed in NB cell lines than that in normal dorsal ganglia and was positively correlated with MYCN expression ($R = 0.48$, $P = 0.0174$, Supplementary Material, Fig. S1D). To further investigate the expression of miR-558, real-time quantitative reverse transcriptase–polymerase chain reaction (RT–PCR) was applied to measure the mature miR-558 levels in 30 NB specimens, normal dorsal ganglia and cultured SK-N-SH, SK-N-AS, SH-SY5Y and SK-N-BE(2) cell lines. As shown in Figure 1B, mature miR-558 was up-regulated in the NB tissues and cell lines compared with normal dorsal ganglia. The western blot assay indicated the high expression of HPSE in NB tissues and cell lines (Fig. 1C). There was a positive correlation between miR-558 expression and *HPSE* transcript levels in NB tissues and cell lines ($R = 0.633$, $P < 0.0001$, Fig. 1D and Supplementary Material, Table S1). Higher miR-558 expression was observed in NB tissues with poor differentiation ($P = 0.0001$, Fig. 1E) or higher HPSE protein levels ($P = 0.0011$, Fig. 1F). These results indicated the up-regulation of miR-558 in NB tissues and cell lines, which was positively correlated with *HPSE* transcript levels.

### miR-558 facilitated HPSE expression through transcriptional activation

To investigate the direct effects of miR-558 on HPSE expression in NB cell lines, we performed the miRNA knockdown and over-expression experiments. Transfection of anti-miR-558 inhibitor into SH-SY5Y and SK-N-BE(2) cells resulted in a decrease in cytoplasmic and nuclear miR-558 levels (Fig. 2A). Western blot, real-time quantitative RT–PCR and nuclear run-on demonstrated that transfection of the anti-miR-558 inhibitor resulted in decreased nascent transcript and protein levels of HPSE in NB cells, when compared with those transfected with the negative control (anti-NC) inhibitor (Fig. 2B–D). The expression levels of *VEGF*, the HPSE downstream target gene (4), were significantly down-regulated in miR-558 knockdown NB cells, consistent with the HPSE reduction (Fig. 2B and C). On the other hand, the stable transfection of the miR-558 precursor into SH-SY5Y and SK-N-SH cells obviously up-regulated the cytoplasmic and nuclear expression of miR-558 (Fig. 2E) and increased the HPSE and VEGF protein levels than those of empty vector-transfected (mock) cells (Fig. 2F). Real-time quantitative RT–PCR and nuclear run-on analyses showed the enhanced transcriptional levels of *HPSE* and *VEGF* in NB cells transfected with the miR-558 precursor, when compared with mock cells (Fig. 2G and H). Since the analysis of the miRNA–promoter interaction database revealed no potential binding site of miR-558 within the *VEGF* promoter (23), we ruled out the possibility that miR-558 may directly regulate the transcription of *VEGF*. In addition, knockdown or over-expression of miR-558 in NB cells did not affect the luciferase activities of *VEGF* 3′-UTR (Supplementary Material,

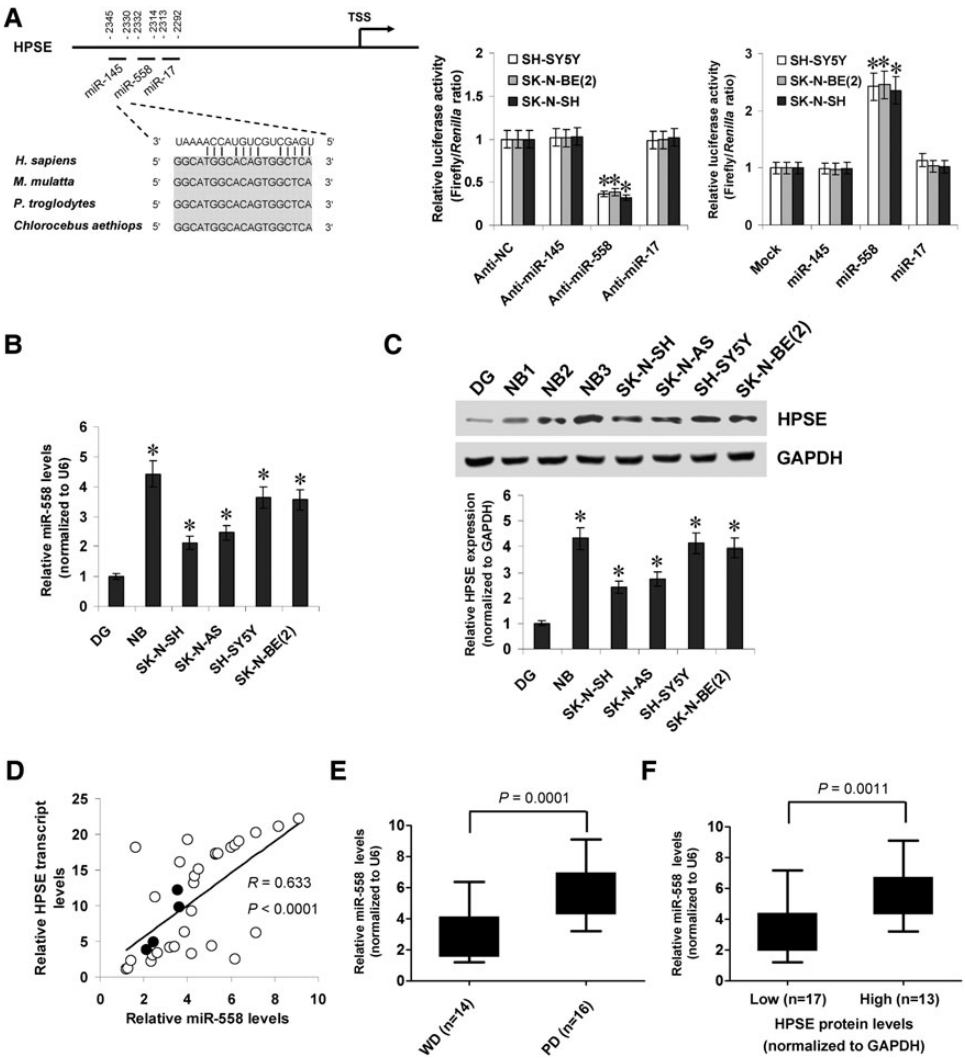


**Figure 1.** MiR-558 was up-regulated and positively correlated with HPSE levels in NB tissues and cell lines. (**A**) The scheme of the potential binding sites of miR-145, miR-558 and miR-17 within the *HPSE* promoter, locating at bases 2330–2345, 2314–2332 and 2292–2313 upstream the TSS. The dual-luciferase assay indicated that the transfection of the miRNA inhibitor or mimic (100 nmol/l) of miR-558, but not of miR-145 or miR-17, altered the promoter activities of *HPSE* in cultured SH-SY5Y, SK-N-BE(2) and SK-N-SH cells, than those transfected with the anti-NC inhibitor or control mimic (mock; $^*P < 0.01$ versus anti-NC or mock). (**B**) Real-time quantitative RT–PCR revealed that miR-558 was up-regulated in NB tissues ($n = 30$) and cell lines [SK-N-SH, SK-N-AS, SH-SY5Y and SK-N-BE(2)] compared with normal dorsal ganglia (DG; $^*P < 0.01$ versus DG). (**C**) The western blot assay indicated the high expression of HPSE in NB tissues and cell lines [SK-N-SH, SK-N-AS, SH-SY5Y and SK-N-BE(2)] than that in DG ($^*P < 0.01$ versus DG). (**D**) There was a positive correlation between miR-558 expression and *HPSE* transcript levels in NB tissues ($n = 30$, white dots) and cell lines ($n = 4$, black dots). (**E**) miR-558 levels were higher in NB tissues with poor differentiation (PD) than those in specimens with well differentiation (WD). (**F**) Higher miR-558 levels were observed in NB tissues with high HPSE expression.

Fig. S2A and B), and no binding site of miR-558 was noted within the 3′-UTR of *HPSE*, indicating no involvement of post-transcription regulation by miR-558. Moreover, restoration of HPSE levels abolished the effects of miR-558 on VEGF expression (Supplementary Material, Fig. S3), indicating that miR-558 regulated the expression of VEGF through modulating HPSE in NB cells. Overall, these results demonstrated that miR-558 considerably facilitated HPSE expression through transcriptional activation.

## miR-558 targeted the binding site and recruited AGO1 on *HPSE* promoter

To determine whether or not miR-558 could promote HPSE expression by targeting its binding site within the *HPSE* promoter, the *HPSE* promoter–luciferase reporter or a mutation of the miRNA seed recognition sequence (Fig. 3A) was transfected into NB cells transfected with anti-miR-558 or anti-NC inhibitors. The firefly luciferase activity normalized to that of *Renilla* was significantly reduced in the tumor cells transfected with the anti-miR-558 inhibitor (Fig. 3B), and the effects were abolished by the mutation of miR-558-binding site within the *HPSE* promoter (Fig. 3B). In addition, the stable transfection of the miR-558 precursor increased the luciferase activities in SH-SY5Y and SK-N-SH cells (Fig. 3C), whereas the mutation of the miR-558 recognition site abolished these effects (Fig. 3C). Since previous studies have revealed the potential involvement of AGO1 and AGO2 in small RNA-induced transcriptional activation (24,25), we next analyzed the binding of AGO1 and AGO2 on the promoter region of *HPSE*. Chromatin immunoprecipitation (ChIP) and real-time quantitative PCR (qPCR) assays indicated that the endogenous

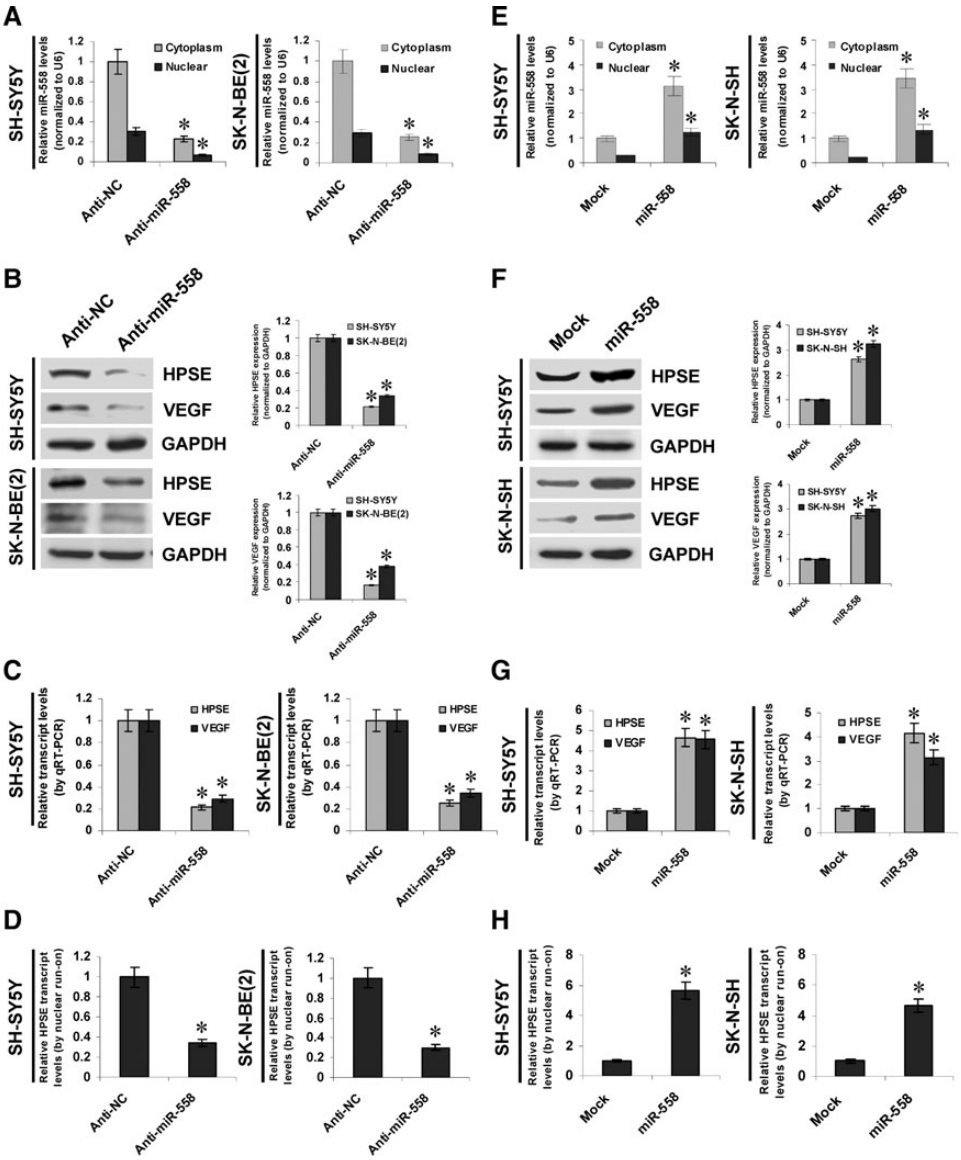


**Figure 2.** MiR-558 facilitated HPSE expression through transcriptional activation. (**A**) Real-time quantitative RT–PCR indicated that the transfection of the anti-miR-558 inhibitor (100 nmol/l) into cultured SH-SY5Y and SK-N-BE(2) cells, resulted in decreased miR-558 levels, when compared with those transfected with the anti-NC inhibitor (100 nmol/l; *$P < 0.01$ versus anti-NC). (**B** and **C**) Western blot and real-time quantitative RT–PCR indicated that the transfection of the anti-miR-558 inhibitor resulted in decreased HPSE and VEGF expression levels in NB cells, when compared with those in anti-NC-transfected cells (*$P < 0.01$ versus anti-NC). (**D**) The nuclear run-on assay indicated the attenuated nascent *HPSE* transcript levels in NB cells transfected with the anti-miR-558 inhibitor, than those of anti-NC-transfected cells (*$P < 0.01$ versus anti-NC). (**E**) Real-time quantitative RT–PCR indicated that the stable transfection of the miR-558 precursor resulted in increased miR-558 levels in SH-SY5Y and SK-N-SH cells, than those transfected with the empty vector (mock; *$P < 0.01$ versus mock). (**F** and **G**) Western blot and real-time quantitative RT–PCR indicated that the stable transfection of the miR-558 precursor increased the HPSE and VEGF levels in SH-SY5Y and SK-N-SH cells, than those in mock cells (*$P < 0.01$ versus mock). (**H**) The nuclear run-on assay indicated the enhanced nascent *HPSE* transcript levels in NB cells stably transfected with miR-558, than those in mock cells (*$P < 0.01$ versus mock).

miR-558-targeting *HPSE* promoter regions were immunoprecipitated using antibody specific for AGO1, but not for AGO2, in cultured SH-SY5Y and SK-N-BE(2) cells, which were 0.33- and 0.23-fold relative to the nuclear extract (input; Fig. 3D). As a control, no *HPSE* promoter region was immunoprecipitated with isotype IgG (Fig. 3D). In addition, knockdown or stable over-expression of miR-558 decreased and increased the binding of AGO1, but not of AGO2, on the *HPSE* promoter, respectively (Fig. 3D and Supplementary Material, Fig. S2C). These results indicated that miR-558 targeted the binding site and recruited AGO1 on the *HPSE* promoter in NB cells.

## Involvement of AGO1 in the miR-558-induced transcriptional activation of *HPSE* in NB cells

To further investigate the potential roles of AGO1 and AGO2 in the miR-558-induced transcriptional activation of *HPSE*, small interfering RNAs (siRNAs) targeting AGO1 and AGO2 were transfected into SH-SY5Y and SK-N-SH cells stably transfected with an empty vector (mock) and the miR-558 precursor, respectively. Western blot, real-time quantitative RT–PCR and nuclear run-on demonstrated that knockdown of AGO1, but not of AGO2, abolished the miR-558-induced transcriptional activation of

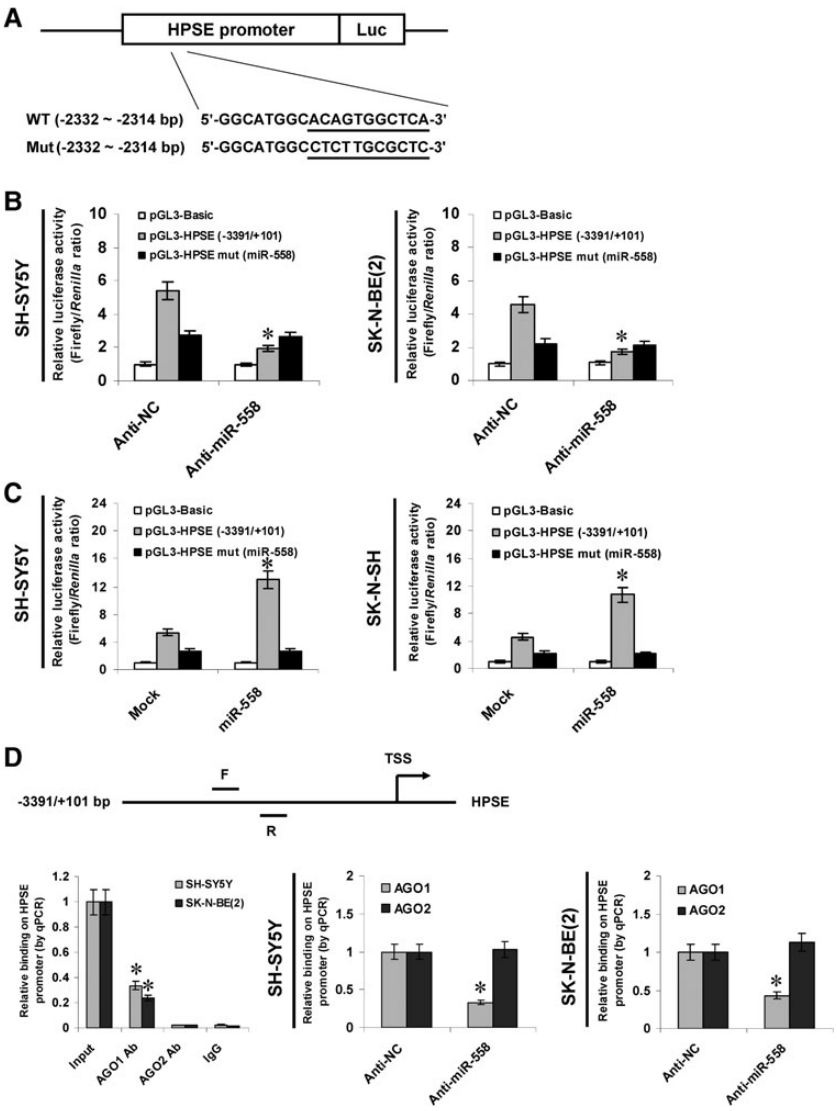


**Figure 3.** MiR-558 targeted the binding site and recruited AGO1 on the *HPSE* promoter. (**A**) The scheme and sequence of the intact miR-558-binding site (WT) and its mutation (Mut) within the *HPSE* promoter luciferase reporter vector. (**B**) Transfection of the anti-miR-558 inhibitor (100 nmol/l) into SH-SY5Y and SK-N-BE(2) cells resulted in decreased luciferase activities of the *HPSE* promoter, when compared with those transfected with the anti-NC inhibitor (100 nmol/l; *$P < 0.01$ versus anti-NC). These effects were abolished by the mutation of the miR-558-binding site within the *HPSE* promoter. (**C**) Stable transfection of the miR-558 precursor into SH-SY5Y and SK-N-SH increased the luciferase activities when compared with those transfected with the empty vector (mock; * $P < 0.01$ versus mock), whereas the mutation of the miR-558 recognition site abolished these effects. (**D**) ChIP and qPCR assays indicated that the endogenous miR-558-targeting *HPSE* promoter regions were immunoprecipitated using antibody (Ab) specific for AGO1, but not for AGO2, in cultured SH-SY5Y and SK-N-BE(2) cells, which were 0.33- and 0.23-fold relative to nuclear extract (input). As a control, no *HPSE* promoter region was immunoprecipitated with isotype IgG. Transfection of the anti-miR-558 inhibitor into SH-SY5Y and SK-N-BE(2) cells resulted in the decreased enrichment of AGO1, but not of AGO2, on the *HPSE* promoter, when compared with that in anti-NC-transfected cells (* $P < 0.01$ versus anti-NC).

*HPSE* in NB cells (Fig. 4A–C). Stable transfection of the miR-558 precursor into NB cells resulted in decreased binding of repressive epigenetic markers histone H3 lysine 9 dimethylation (H3K9me2) and histone H3 lysine 27 trimethylation (H3K27me3) and increased binding of the active epigenetic marker histone H3 lysine 4 trimethylation (H3K4me3) and RNA polymerase II (RNA Pol II) on the *HPSE* promoter (Fig. 4D), which was abolished by the knockdown of AGO1 (Fig. 4D). To explore whether miR-558 interacts directly with the *HPSE* promoter, lysates from miR-558 over-expressing NB cells were pretreated with RNase H or RNase A. As shown in Figure 4E, RNase H treatment prevented the NB cells from the increased enrichment of AGO1, H3K4me3 and RNA Pol II and decreased binding of H3K9me2 and H3K27me3 on the *HPSE* promoter induced by miR-558. However, these changes were unaffected by RNase A treatment (Fig. 4E), indicating a direct interaction between miR-558 and the *HPSE* promoter. Collectively, these results indicated that miR-558 induced chromatin remodeling within the *HPSE* promoter in NB cells in an AGO1-dependent manner.

## miR-558 promoted the growth, invasion, metastasis and angiogenesis of NB cells through targeting HPSE *in vitro*

Since previous studies indicate that HPSE promotes the growth, migration, invasion and angiogenesis of tumor cells (11), we further investigated the effects of miR-558 knockdown and HPSE

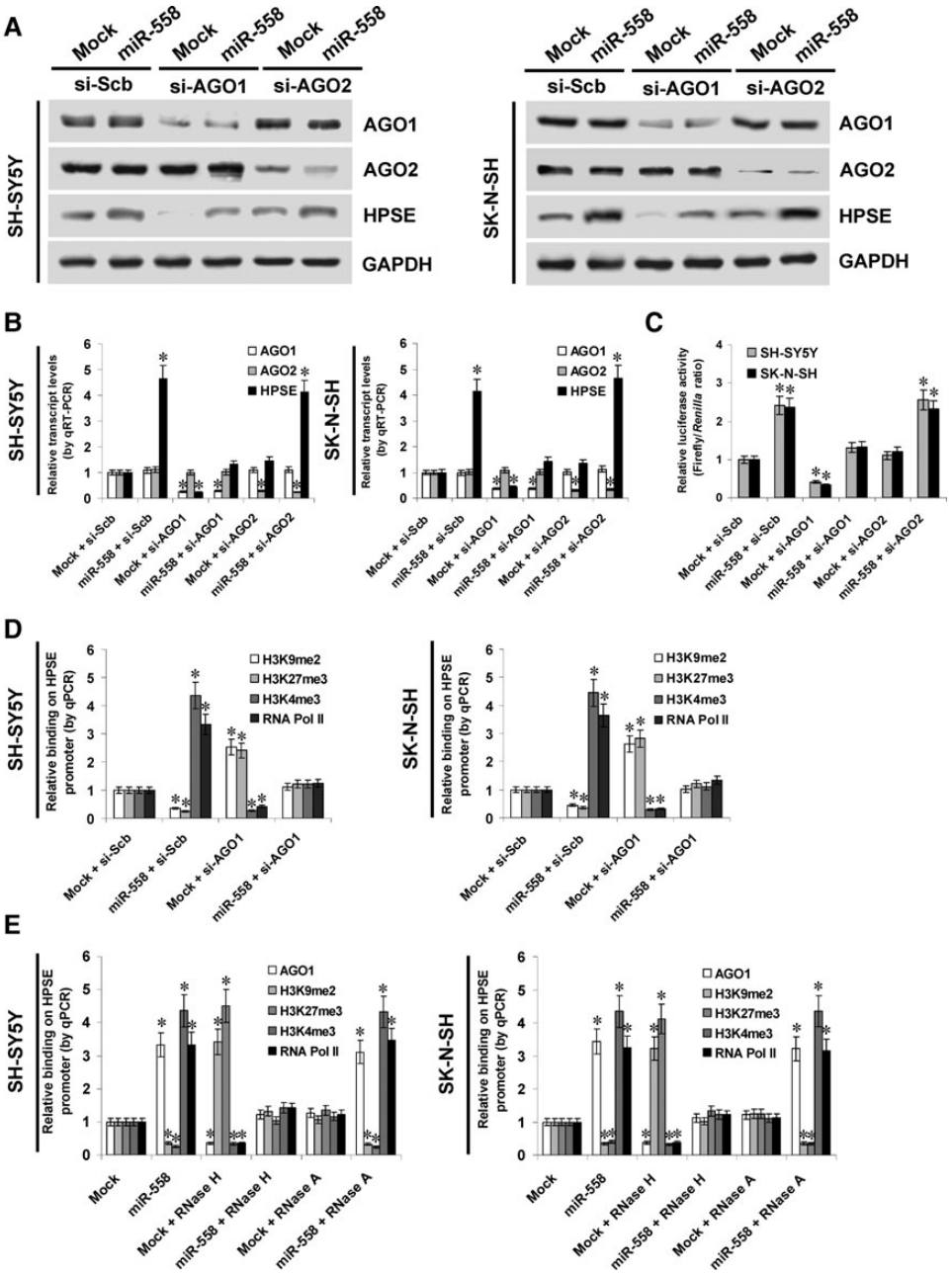


**Figure 4.** AGO1 was involved in the miR-558-induced transcriptional activation of *HPSE* in NB cells. (**A** and **B**) Western blot and real-time quantitative RT–PCR assays indicated that the transfection of siRNA-targeting AGO1 (si-AGO1, 100 nmol/l), but not siRNA-targeting AGO2 (si-AGO2, 100 nmol/l), abolished the miR-558-induced HPSE expression in SH-SY5Y and SK-N-SH cells, than those transfected with the empty vector (mock) and si-Scb (*$P < 0.01$ versus mock + si-Scb). (**C**) The nuclear run-on assay indicated that the transfection of si-AGO1 (100 nmol/l), but not of si-AGO2 (100 nmol/l), attenuated the miR-558-induced nascent *HPSE* transcription in NB cells, than those transfected with mock and si-Scb (*$P < 0.01$ versus mock + si-Scb). (**D**) ChIP and qPCR assays indicated that the stable transfection of the miR-558 precursor into NB cells resulted in decreased binding of H3K9me2 and H3K27me3 and increased enrichment of H3K4me3 and RNA Pol II on the *HPSE* promoter, than those transfected with the empty vector (mock). Transfection of si-AGO1 (100 nmol/l) attenuated the miR-558-induced these changes in NB cells, than those transfected with si-Scb (*$P < 0.01$ versus mock + si-Scb). (**E**) RNase H treatment prevented the SH-SY5Y and SK-N-SH cells from increased enrichment of AGO1, H3K4me3 and RNA Pol II and decreased binding of H3K9me2 and H3K27me3 on the *HPSE* promoter induced by miR-558. However, these changes were unaffected by RNase A treatment (*$P < 0.01$ versus mock).

restoration on cultured NB cells. Western blot indicated that the transfection of *HPSE* rescued the miR-558 knockdown-induced down-regulation of HPSE and VEGF (Fig. 5A). In 2-(4,5-dimethyltriazol-2-yl)-2,5-diphenyl tetrazolium bromide (MTT) colorimetric and soft agar assays, tumor cells transfected with the anti-miR-558 inhibitor possessed the decreased viability and growth capabilities, when compared with those transfected with the anti-NC inhibitor (Fig. 5B and C and Supplementary Material, Fig. S4A). In the scratch migration assay, miR-558 knockdown attenuated the migration capabilities of SH-SY5Y and SK-N-BE(2) cells (Fig. 5D and Supplementary Material, Fig. S4B). Transwell analysis showed that NB cells transfected with the anti-miR-558 inhibitor presented an impaired invasion capacity than that in anti-NC-transfected cells (Fig. 5E). The

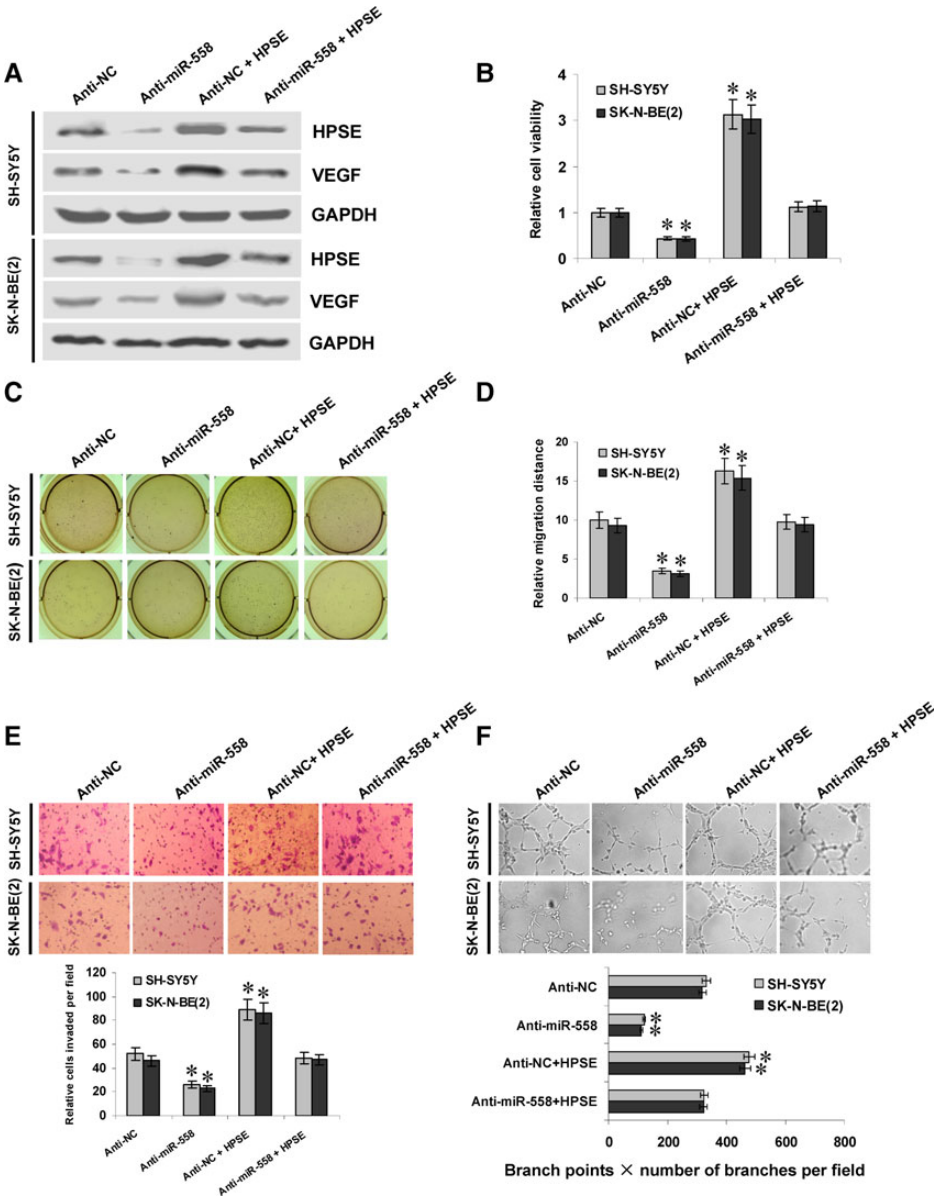


**Figure 5.** Knockdown of miR-558 suppressed the growth, migration, invasion and angiogenesis of NB cells *in vitro*. (**A**) Western blot indicated that the transfection of *HPSE* restored the down-regulation of HPSE and VEGF induced by miR-558 knockdown. (**B** and **C**) MTT colorimetric and soft agar assays indicated that the viability and growth of NB cells were decreased by miR-558 knockdown, and the transfection of *HPSE* rescued these changes (*$P < 0.01$ versus anti-NC). (**D**) In the scratch migration assay, the migration of miR-558 knockdown NB cells was significantly reduced. Transfection of *HPSE* rescued the migration of miR-558 knockdown cells (*$P < 0.01$ versus anti-NC). (**E**) The matrigel invasion assay indicated the decreased invasion capabilities in miR-558 knockdown cells. However, the transfection of *HPSE* restored the invasion of miR-558 knockdown cells (*$P < 0.01$ versus anti-NC). (**F**) The tube formation of endothelial HUVEC cells was suppressed by treatment with the medium preconditioned by miR-558 knockdown cells, when compared with that of anti-NC-transfected cells. Restoration of HPSE expression rescued the angiogenic capabilities of miR-558 knockdown cells (*$P < 0.01$ versus anti-NC).

tube formation of endothelial cells was suppressed by treatment with the medium preconditioned by the transfection of NB cells with the anti-miR-558 inhibitor (Fig. 5F). In addition, the transfection of *HPSE* into SH-SY5Y and SK-N-BE(2) cells restored the decrease in growth, migration, invasion and angiogenesis induced by knockdown of miR-558 (Fig. 5B–F and Supplementary Material, Fig. S4). On the other hand, we examined the effects of miR-558 over-expression on NB cells. Stable transfection of the miR-558 precursor into SH-SY5Y and SK-N-SH cells resulted in the enhanced expression of HPSE and VEGF (Supplementary Material, Fig. S5A) and increased capabilities in cell viability (Supplementary Material, Fig. S5B), growth (Supplementary Material, Fig. S5C), migration (Supplementary Material, Fig. S5D), invasion (Supplementary Material, Fig. S5E) and angiogenesis (Supplementary Material, Fig. S5F). In addition, restoration of HPSE expression via transfection of siRNA specific for *HPSE* rescued the NB cells from their changes in these biological features induced by stable over-expression of miR-558 (Supplementary Material, Fig. S5). Meanwhile, restoration of VEGF levels only partially prevented the NB cells from miR-558-mediated changes in the growth, migration, invasion and angiogenesis *in vitro* (Supplementary Material, Fig. S6). These results indicated that miR-558 remarkably promoted the growth, migration, invasion and angiogenesis of NB cells through targeting HPSE *in vitro*.

### Knockdown of miR-558 attenuated the growth, metastasis and angiogenesis of NB cells *in vivo*

We next investigated the efficacy of miR-558 knockdown against tumor growth, metastasis and angiogenesis *in vivo*. Administration of the anti-miR-558 inhibitor via tail vein injection decreased the growth and tumor weight of SH-SY5Y cells-established subcutaneous xenograft tumors in athymic nude mice, when compared with those treated with anti-NC (Fig. 6A and B). In addition, immunohistochemical staining, western blot and real-time quantitative RT-PCR indicated that the expression of HPSE and downstream VEGF was also reduced by the knockdown of miR-558 via the administration of the anti-miR-558 inhibitor (Fig. 6C and D). Moreover, treatment with the anti-miR-558 inhibitor resulted in decrease in CD31-positive microvessels and mean vessel density within tumors (Fig. 6C). In the experimental metastasis studies, nude mice treated with the anti-miR-558 inhibitor established statistically fewer lung metastatic colonies than those treated with anti-NC (Fig. 6E). These results suggested that knockdown of miR-558 inhibited the growth, metastasis and angiogenesis of NB cells *in vivo*.

## Discussion

The human *HPSE* gene is located at chromosome 4q21.3, and its expression is regulated at the transcriptional levels (26).

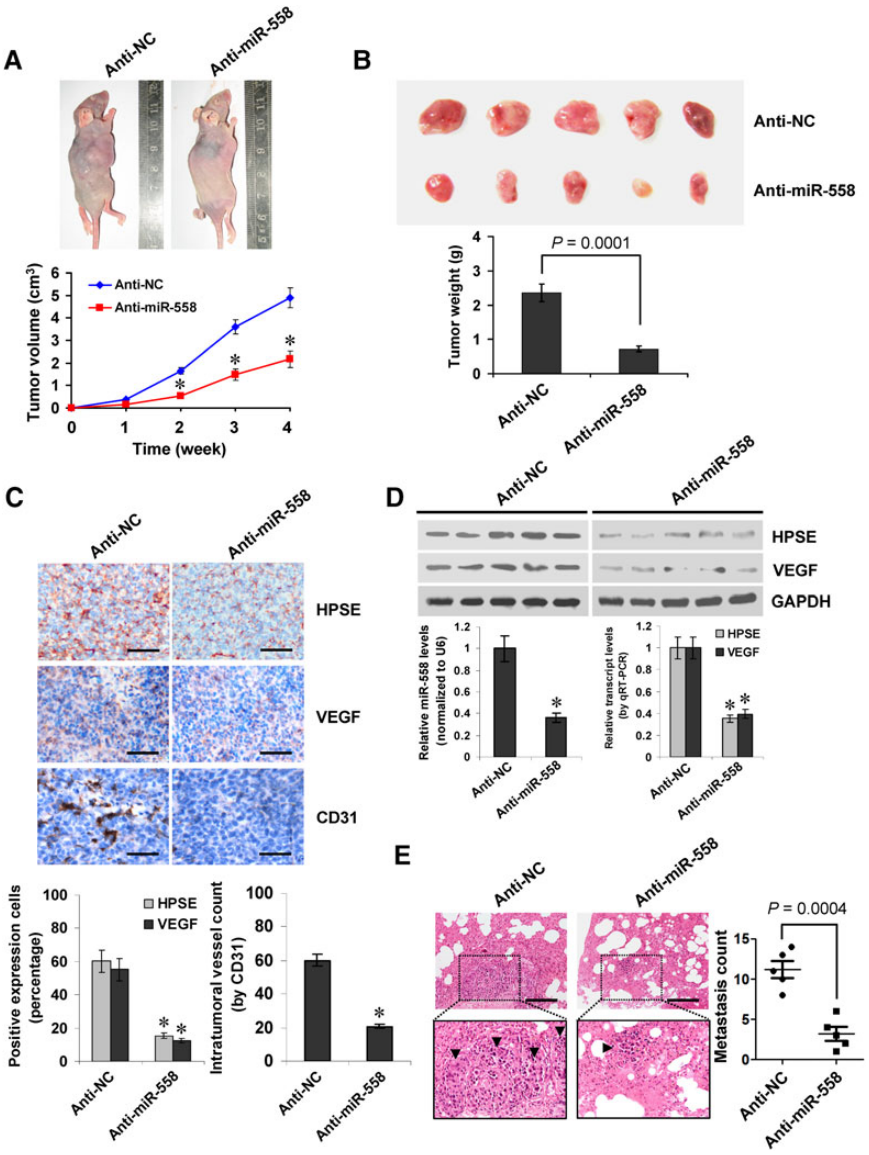


**Figure 6.** Knockdown of miR-558 attenuated the growth, metastasis and angiogenesis of NB cells *in vivo*. (**A** and **B**) Hypodermic injection of SH-SY5Y cells into athymic nude mice established subcutaneous xenograft tumors. Four weeks later, mice ($n = 5$) from each group were sacrificed. Administration of the anti-miR-558 inhibitor (10 μmol/l in 0.1 ml of PBS) via tail vein injection resulted in decreased tumor growth than that of anti-NC (*$P < 0.01$ versus anti-NC), and the mean tumor weight was significantly decreased. (**C**) Immunohistochemical staining revealed that administration of the anti-miR-558 inhibitor resulted in decreased expression of HPSE, VEGF and CD31 within tumors. The mean vessel density within tumors decreased after treatment with the anti-miR-558 inhibitor (*$P < 0.01$ versus anti-NC). Scale bars: 100 μm. (**D**) Western blot and real-time quantitative RT–PCR indicated that the expression of HPSE and VEGF was reduced by knockdown of miR-558 via administration of the anti-miR-558 inhibitor (*$P < 0.01$ versus anti-NC). (**E**) SH-SY5Y cells were injected into the tail vein of athymic nude mice ($0.4 \times 10^6$ cells per mouse, $n = 5$ for each group). The nude mice treated with the anti-miR-558 inhibitor (10 μmol/l in 0.1 ml of PBS) established significantly fewer lung metastatic colonies (arrowheads). Scale bars: 100 μm.

In non-cancerous tissues and cells, HPSE is constitutively inhibited, and it is over-expressed in essentially all human tumors examined (3). Transcription factors specificity protein 1 and v-ets avian erythroblastosis virus E26 oncogene homolog are associated with the basal activity of the *HPSE* promoter (27,28), whereas early growth response 1 is implicated in the inducible transcription of *HPSE* (29). Estrogen exposure enhances the *HPSE* promoter activities through four estrogen response elements in breast cancer cells (30). Wild-type p53 has been shown to inhibit the *HPSE* transcription by direct binding to its promoter (31). In this study, we demonstrate that miR-558 facilitates the HPSE expression in NB cells. First, the expression of miR-558 and HPSE was positively correlated in NB tissues and cell lines. Second, the activities of the *HPSE* promoter luciferase reporter were responsive to miR-558 knockdown and over-expression. Third, the mutation of the miR-558-binding site abolished the regulatory effects of miR-558 on the *HPSE* promoter luciferase reporter. Finally, the endogenous HPSE expression, both nascent transcript and protein, was increased in miR-558 precursor-transfected NB cells, suggesting that miR-558 may regulate *HPSE* expression by inducing transcription.

Previous studies have shown that promoter-targeting siRNAs can direct transcriptional activation of E-cadherin (24), $p21^{WAF/CIP1}$(24), VEGF (24) and the progesterone receptor (32) in cancer cells. Recent studies reveal the existence of nuclear AGO proteins and miRNA-AGO coupling (33,34). Nuclear-cytoplasmic proteins, such as trinucleotide repeat containing 6A, interact with AGO proteins for nuclear internalization (33,34). The miRNA-binding sites within promoters are present as commonly as those within 3′-UTRs (35). In human nasopharyngeal carcinoma cells, 39 miRNAs are identified in the nuclear fractions (36). Within the E-cadherin promoter, there is a miR-373 target site, and transfection of miR-373 precursor activates the E-cadherin expression in prostate cancer cells (17), providing the first evidence that promoter-targeting miRNAs can elicit transcriptional activation. Subsequent studies show that miR-205 functions as a tumor suppressor through up-regulating interleukin-24 and interleukin-32 by targeting specific sites in their promoters (37). In addition, miR-744 activates cyclin B1 transcription by binding its promoter in an AGO1-dependent manner, involving increased recruitment of H3K4me3 and RNAP II on the *cyclin B1* promoter (25). In this study, we found that in miR-558 over-expressing NB cells, the recruitment of repressive epigenetic markers H3K9me2 and H3K27me3 was decreased, accompanied by increased enrichment of H3K4me3 and RNA Pol II on the *HPSE* promoter, indicating that miR-558 induces chromatin remodeling that facilitates the transcription of *HPSE* in NB cells.

MiR-558, a recently identified miRNA in human colorectal cells, is found to be up-regulated in irradiated fibroblasts (38) and regulates target genes involved in cell cycle checkpoints and apoptosis (39). Over-expression of miR-558 markedly inhibits the interleukin-1 beta-induced production of cyclooxygenase-2 and prostaglandin E2 in human articular chondrocytes (40). In breast cancer tissues, miR-558 is significantly down-expressed (41). In this study, we identified the up-regulation of miR-558 in NB tissues and cell lines than that in normal dorsal ganglia and noted the high expression of BIRC6, the host gene of miR-558, in a publicly available NB microarray database. It has been shown that miR-558 exerts oncogenic functions to increase the *in vitro* proliferation, colony formation and *in vivo* growth of NB cells (22). However, the other oncogenic functions of miR-558 and underlying mechanisms in NB still remain largely unknown. In this study, we demonstrate that miR-558 facilitates the growth of NB cells, which is in line with previous studies (22). In addition, our evidence shows that miR-558 promotes the invasion, metastasis and angiogenesis of NB cells *in vitro* and *in vivo*. The fact that the restoration of HPSE expression is sufficient to prevent the NB cells from miR-558-mediated changes in these biological features suggests that miR-558 exerts the oncogenic functions, at least in part, through up-regulation of HPSE in NB. Moreover, rescue experiments show that VEGF partially contributes to the miR-558-mediated oncogenic effects, suggesting the involvement of other downstream genes of HPSE in these processes.

Transcription regulation depends on the interactions between repressor or activator proteins with promoter sequences, and miRNA-AGO complexes may activate transcription through epigenetic mechanisms (42). In this study, our evidence indicated that AGO1, but not AGO2, was enriched at the *HPSE* promoter in miR-558 over-expressing NB cells. In addition, the knockdown of AGO1 abolished the miR-558-induced binding of an active epigenetic marker on the *HPSE* promoter. We believe that miR-558/AGO1 complexes may recruit co-activator such as histone methyltransferases to facilitate gene expression, which warrants our further investigation. Because RNA is able to form base pairs with DNA, it is reasonable to suspect that miRNAs may directly hybridize with regulatory regions within genomic DNA (42). When promoters are in single-stranded open conformation, miRNA-binding sites may be achieved (42). In this study, we found that treatment with RNase H (specifically degrades the RNA present in RNA-DNA hybrid) (18) attenuated the miR-558-induced changes in the enrichment of AGO1 and epigenetic markers, suggesting a direct interaction between miR-558 and the *HPSE* promoter.

In summary, we have shown that miR-558 is up-regulated in human NB and facilitates the transcription of *HPSE* via the binding site within its promoter in NB cell lines. Furthermore, miR-558 promotes the growth, invasion, metastasis and angiogenesis of NB cells *in vitro* and *in vivo* through up-regulating HPSE expression. This study extends our knowledge about the regulation of *HPSE* at the transcriptional level by miRNAs and suggests that miR-558 may be of potential values as a novel therapeutic target for human NB.

## Materials and Methods

### Patient tissue samples

Approval to conduct this study was obtained from the Institutional Review Board of Tongji Medical College (approval number: 2011-S085). Fresh tumor specimens from 30 well-established primary NB cases were collected at surgery and stored at –80°C until use. The pathological diagnosis of NB was confirmed by at least two pathologists. Based on the Shimada classification system, including the mitosis karyorrhexis index, degree of neuroblastic differentiation and stromal maturation and patient's age, 14 patients were classified as having favorable histology and 16 as having unfavorable histology. According to the INSS, four patients were classified as stage 1, nine as stage 2, nine as stage 3, four as stage 4 and four as stage 4S. Protein and RNAs of normal human dorsal ganglia were obtained from Clontech (Mountain View, CA, USA).

### Promoter-targeted miRNA prediction and expression detection

miRNA-binding sites within the *HPSE* promoter were predicted using the algorithm microPIR (21) and the genome-wide profiling

of AGO–chromosome interaction data (GSE40536). Cytoplasmic and nuclear fractions were prepared using the NE-PER Nuclear and Cytoplasmic Extraction Reagents (Thermo Fisher Scientific, Inc., Waltham, MA, USA). The levels of mature miRNA in primary tissues and cell lines were determined using Bulge-Loop™ miRNAs qPCR Primer Set (RiboBio Co. Ltd, Guangzhou, China). After cDNA was synthesized with a miRNA-specific stem-loop primer, the qPCR was performed with the specific primers (Supplementary Material, Table S2). The miRNA levels were normalized as to those of U6 snRNA.

### Western blot

Tissue or cellular protein was extracted with a 1 × cell lysis buffer (Promega, Madison, WI, USA). Western blot was performed as previously described (43–47), with antibodies specific for HPSE (Abcam Inc., Cambridge, MA, USA), VEGF (Santa Cruz Biotechnology, Santa Cruz, CA, USA), AGO1 (Cell Signaling Technology, Inc., Danvers, MA, USA), AGO2 (Cell Signaling Technology, Inc.) and glyceraldehyde-3-phosphate dehydrogenase (Santa Cruz Biotechnology). The ECL substrate kit (Amersham, Piscataway, NJ, USA) was used for the chemiluminscent detection of signals with autoradiography film (Amersham).

### Real-time quantitative RT–PCR

Total RNA was isolated with the RNeasy Mini Kit (Qiagen Inc., Valencia, CA, USA). The RT reactions were conducted with the Transcriptor First Strand cDNA Synthesis Kit (Roche, Indianapolis, IN, USA). Real-time PCR was performed with SYBR Green PCR Master Mix (Applied Biosystems, Foster City, CA, USA) and primers listed in Supplementary Material, Table S2. The fluorescent signals were collected during the extension phase, Ct values of the sample were calculated and the transcript levels were analyzed by the $2^{-\triangle\triangle Ct}$ method.

### Cell culture and transfection

Human NB cell lines SK-N-SH (HTB-11), SK-N-AS (CRL-2137), SH-SY5Y (CRL-2266) and SK-N-BE(2) (CRL-2271) and the human endothelial cell line HUVEC (CRL-1730) were purchased from American Type Culture Collection (Rockville, MD, USA). Cell lines were authenticated on the basis of viability, recovery, growth, morphology and isoenzymology by the provider. Cell lines were used within 6 months after the resuscitation of frozen aliquots and grown in the RPMI1640 medium (Life Technologies, Inc., Gaithersburg, MD, USA) supplemented with 10% fetal bovine serum (Life Technologies, Inc.), penicillin (100 U/ml) and streptomycin (100 µg/ml). Cells were maintained at 37°C in a humidified atmosphere of 5% $CO_2$. The miRNA inhibitors (antagomiR oligos) and mimics of miR-145, miR-558, miR-17 or anti-NC (RiboBio Co. Ltd) were transfected into confluent cells with Lipofectamine 2000 (Life Technologies, Inc.).

### Pre-miRNA construct and stable transfection

According to the pre-miR-558 (5′-TGAGCTGCTGTACCAAAAT-3′) sequence documented in the miRNA Registry database (48), oligonucleotides encoding the precursor of miR-558 (Supplementary Material, Table S3) were subcloned into the *Bam*HI and *Xho*I restrictive sites of pcDNA3.1(–) (Genechem Co., Ltd, Shanghai, China). The miR-558 expression vector was transfected into tumor cells, and stable cell lines were screened by the administration of neomycin (Invitrogen, Carlsbad, CA). The empty vector was applied as a control.

### Luciferase reporter assay

The human *HPSE* promoter luciferase reporter was kindly provided by Dr Xiulong Xu (Rush University Medical Center) (11,27). The mutation of the miR-558-binding site was performed with GeneTailor™ Site-Directed Mutagenesis System (Invitrogen) and PCR primers (Supplementary Material, Table S3). Tumor cells were plated at $1 \times 10^5$ cells/well on 24-well plates and transfected by luciferase reporter vectors (30 ng) and a *Renilla* luciferase reporter vector pRL-SV40 (10 ng, Promega). Twenty-four hours post-transfection, firefly and *Renilla* luciferase activities were consecutively measured, according to the dual-luciferase assay manual (Promega). For *HPSE* promoter activities, the luciferase signal was normalized by the firefly/*Renilla* ratio.

### Nuclear run-on assay

The nuclear run-on assay was performed based on the incorporation of biotin-16-uridine-5′-triphosphate (biotin-16-UTP) in nascent transcripts as described previously (11). Briefly, nuclei of $5 \times 10^6$ tumor cells were isolated and consequently incubated in a reaction buffer containing rNTPs and biotin-16-UTP (Roche) at 30°C for 45 min. The reaction was stopped by adding RNase-free DNase I (Sigma, St Louis, MO, USA), and the nuclei were lysed and treated with proteinase K (Sigma). Total RNA was extracted using Trizol (Invitrogen), and biotinylated nascent RNA was purified using agarose-conjugated streptavidin beads (Invitrogen). Beads were then eluted, and biotinylated RNA was isolated for the real-time quantitative RT–PCR assay with primers (Supplementary Material, Table S2).

### Gene over-expression and knockdown

Human *HPSE* cDNA (1632 bp) and *VEGF* cDNA (1116 bp) were amplified from the NB tissue (Supplementary Material, Table S3) and subcloned into pcDNA3.1 (Invitrogen). To restore the miR-558 knockdown-induced down-regulation of HPSE or VEGF, tumor cell lines were transfected with the recombinant vector pcDNA3.1-HPSE or pcDNA3.1-VEGF. The 21-nucleotide siRNAs targeting the encoding region of *HPSE* (11), *AGO1* (11), *AGO2* (11) and *VEGF* were chemically synthesized (RiboBio Co. Ltd) and transfected into tumor cells stably over-expressing miR-558 with Genesilencer Transfection Reagent (Genlantis, San Diego, CA, USA). The scramble siRNA (si-Scb) was applied as a control (Supplementary Material, Table S3).

### Chromatin immunoprecipitation

The ChIP assay was performed according to the manufacturer's instructions of the EZ-ChIP kit (Upstate Biotechnology, Temacula, CA, USA) (11,45,49), with antibodies for AGO1, AGO2, H3K9me2, H3K27me3, H3K4me3 and RNA Pol II (Upstate Biotechnology). Lysates were treated with either RNase H (10 U) or RNase A (20 µg) prior to immunoprecipitation. DNA was sonicated into fragments of an average size of 200 bp. Real-time qPCR was performed with primers targeting the binding site of miR-558 within the *HPSE* promoter (Supplementary Material, Table S2).

### Cell viability assay

Tumor cells were cultured in 96-well plates at $5 \times 10^3$ cells per well. Cell viability was monitored by the MTT (Sigma) colorimetric assay (11,49). All experiments were done with 6–8 wells per experiment and repeated at least three times.

### Soft agar assay

Tumor cells at $5 \times 10^3$ per well were mixed with 0.05% Nobel agar (Fisher Scientific, Pittsburgh, PA, USA) in the growth medium and plated onto 6-well plates containing a solidified bottom layer (0.1% Noble agar in the growth medium). After the incubation of cells for 21 days, the number of cell colonies was counted under the microscope, and the cells were fixed with 100% methanol and stained with 0.5% crystal violet dye (44,45).

### Scratch migration assay

Tumor cells were cultured in 24-well plates and scraped with the fine end of 1-ml pipette tips (time 0). Plates were washed twice with phosphate-buffered saline (PBS) to remove detached cells and incubated with the complete growth medium. Cell migration was photographed using 10 high-power fields, at 0 and 24 h post-induction of injury. Remodeling was measured as diminishing distance across the induced injury, normalized to the 0 h control, and expressed as outgrowth (μm) (43,46,49).

### Cell invasion assay

The matrigel invasion assay was performed using membranes coated with the matrigel matrix (BD Science, Sparks, MD, USA). Homogeneous single cell suspensions ($1 \times 10^5$ cells/well) were added to the upper chambers and allowed to invade for 24 h at 37°C in a $CO_2$ incubator. Invaded cells were stained with 0.1% crystal violet for 10 min at room temperature and examined by light microscopy. Quantification of invaded cells was performed according to the published criteria (43,44,46,47,49).

### Tube formation assay

Fifty microliters of growth factor-reduced matrigel was polymerized on 96-well plates. HUVECs were serum starved in the RPMI1640 medium for 24 h, suspended in the RPMI1640 medium preconditioned with tumor cells, added to the matrigel-coated wells at the density of $5 \times 10^4$ cells/well and incubated at 37°C for 18 h. Quantification of angiogenic activity was calculated by measuring the length of tube walls formed between discrete endothelial cells in each well relative to the control (43,44,46,49).

### *In vivo* growth, metastasis and angiogenesis assay

All animal experiments were approved by the Animal Care Committee of Tongji Medical College (approval number: Y20080290). For the *in vivo* tumor growth studies, 2-month-old male nude mice ($n = 5$ per group) were injected subcutaneously in the upper back with $1 \times 10^6$ tumor cells. Anti-NC or miR-558 antagomiR (10 μmol/l in 0.1 ml of PBS) was administered via tail vein injection 2 days after implantation (50). One month later, mice were sacrificed and examined for tumor weight, gene expression and angiogenesis. The experimental metastasis ($0.4 \times 10^6$ tumor cells per mouse, $n = 5$ per group) studies were performed with 2-month-old male nude mice as described previously (43–45,50).

### Immunohistochemistry

Immunohistochemical staining was performed as previously described (10,43–45), with antibodies specific for HPSE (Abcam Inc.; Santa Cruz Biotechnology; 1:200 dilution), VEGF and CD31 (Santa Cruz Biotechnology; 1:200 dilutions). The immunoreactivity in each tissue section was assessed by at least two pathologists. The degree of positivity was determined according to the percentage of positive tumor cells.

### Statistical analysis

Unless otherwise stated, all data were shown as mean ± standard error of the mean (SEM). The SPSS 18.0 statistical software (SPSS Inc., Chicago, IL, USA) was applied for statistical analysis. The $\chi^2$ analysis and Fisher's exact probability analysis were applied for comparison among the miR-558 expression and individual clinicopathological features. Pearson's coefficient correlation was applied for analyzing the relationship between miR-558 and *HPSE* transcript levels. Difference of tumor cells was determined by the *t*-test or analysis of variance (ANOVA).

## Supplementary Material

Supplementary Material is available at *HMG* online.

## Acknowledgements

We are grateful for Xiulong Xu for providing the *HPSE* promoter luciferase vector.

*Conflict of Interest statement*. None declared.

## Funding

This work was supported by the National Natural Science Foundation of China (81101905, 81272779, 81372667, 81372401, 81472363, 81402301, 81402408), Fundamental Research Funds for the Central Universities (2012QN224, 2013ZHYX003, 01-18-530112, 01-18-530115) and Natural Science Foundation of Hubei Province (2014CFA012).

## References

1. Westermann, F. and Schwab, M. (2002) Genetic parameters of neuroblastomas. *Cancer Lett.*, **184**, 127–147.
2. Israel, V., Neta, I., Annamaria, N. and Benito, C. (2007) Heparanase: structure, biological functions, and inhibition by heparin-derived mimetics of heparan sulfate. *Curr. Pharm. Des.*, **13**, 2057–2073.
3. Ramani, V.C., Purushothaman, A., Stewart, M.D., Thompson, C.A., Vlodavsky, I., Au, J.L. and Sanderson, R.D. (2013) The heparanase/syndecan-1 axis in cancer: mechanisms and therapies. *FEBS J.*, **280**, 2294–2306.
4. Zetser, A., Bashenko, Y., Edovitsky, E., Levy-Adam, F., Vlodavsky, I. and Ilan, N. (2006) Heparanase induces vascular endothelial growth factor expression: correlation with p38 phosphorylation levels and Src activation. *Cancer Res.*, **66**, 1455–1463.
5. Sato, T., Yamaguchi, A., Goi, T., Hirono, Y., Takeuchi, K., Katayama, K. and Matsukawa, S. (2004) Heparanase expression in human colorectal cancer and its relationship to tumor angiogenesis, hematogenous metastasis, and prognosis. *J. Surg. Oncol.*, **87**, 174–181.
6. Koliopanos, A., Friess, H., Kleeff, J., Shi, X., Liao, Q., Pecker, I., Vlodavsky, I., Zimmermann, A. and Büchler, M.W. (2001) Heparanase expression in primary and metastatic pancreatic cancer. *Cancer Res.*, **61**, 4655–4659.
7. Heukamp, L.C., van der Burg, S.H., Drijfhout, J.W., Melief, C.J., Taylor-Papadimitriou, J. and Offringa, R. (2001) Identification of three non-VNTR MUC1-derived HLA-A*0201-restricted

T-cell epitopes that induce protective anti-tumor immunity in HLA-A2/K(b)- transgenic mice. *Int. J. Cancer*, **91**, 385–392.
8. Takaoka, M., Naomoto, Y., Ohkawa, T., Uetsuka, H., Shirakawa, Y., Uno, F., Fujiwara, T., Gunduz, M., Nagatsuka, H., Nakajima, M. *et al.* (2003) Heparanase expression correlates with invasion and poor prognosis in gastric cancers. *Lab. Invest.*, **83**, 613–622.
9. Shinyo, Y., Kodama, J., Hongo, A., Yoshinouchi, M. and Hiramatsu, Y. (2003) Heparanase expression is an independent prognostic factor in patients with invasive cervical cancer. *Ann. Oncol.*, **14**, 1505–1510.
10. Zheng, L.D., Tong, Q.S., Tang, S.T., Du, Z.Y., Liu, Y., Jiang, G.S. and Cai, J.B. (2009) Expression and clinical significance of heparanase in neuroblastoma. *World J. Pediatr.*, **5**, 206–210.
11. Jiang, G., Zheng, L., Pu, J., Mei, H., Zhao, J., Huang, K., Zeng, F. and Tong, Q. (2012) Small RNAs targeting transcription start site induce heparanase silencing through interference with transcription initiation in human cancer cells. *PLoS ONE*, **7**, e31379.
12. Zheng, L., Jiang, G., Mei, H., Pu, J., Dong, J., Hou, X. and Tong, Q. (2010) Small RNA interference-mediated gene silencing of heparanase abolishes the invasion, metastasis and angiogenesis of gastric cancer cells. *BMC Cancer*, **10**, 33.
13. Mei, H., Lin, Z.Y. and Tong, Q.S. (2014) The roles of microRNAs in neuroblastoma. *World J. Pediatr.*, **10**, 10–16.
14. Bartel, D.P. (2004) MicroRNAs: genomics, biogenesis, mechanism, and function. *Cell*, **116**, 281–297.
15. Tay, Y., Zhang, J., Thomson, A.M., Lim, B. and Rigoutsos, I. (2008) MicroRNAs to Nanog, Oct4 and Sox2 coding regions modulate embryonic stem cell differentiation. *Nature*, **455**, 1124–1128.
16. Zhang, L., Sullivan, P.S., Goodman, J.C., Gunaratne, P.H. and Marchetti, D. (2011) MicroRNA-1258 suppresses breast cancer brain metastasis by targeting heparanase. *Cancer Res.*, **71**, 645–654.
17. Place, R.F., Li, L.C., Pookot, D., Noonan, E.J. and Dahiya, R. (2008) MicroRNA-373 induces expression of genes with complementary promoter sequences. *Proc. Natl Acad. Sci. USA*, **105**, 1608–1613.
18. Younger, S.T. and Corey, D.R. (2011) Transcriptional gene silencing in mammalian cells by miRNA mimics that target gene promoters. *Nucleic Acids Res.*, **39**, 5682–5691.
19. Tan, Y., Zhang, B., Wu, T., Skogerbo, G., Zhu, X., Guo, X., He, S. and Chen, R. (2009) Transcriptional inhibiton of Hoxd4 expression by miRNA-10a in human breast cancer cells. *BMC Mol. Biol.*, **10**, 12.
20. Kim, D.H., Sætrom, P., Snøve, O. and Rossi, J.J. (2008) MicroRNA-directed transcriptional gene silencing in mammalian cells. *Proc. Natl Acad. Sci. USA*, **105**, 16230–16235.
21. Piriyapongsa, J., Bootchai, C., Ngamphiw, C. and Tongsima, S. (2012) microPIR: an integrated database of microRNA target sites within human promoter sequences. *PLoS ONE*, **7**, e33888.
22. Shohet, J.M., Ghosh, R., Coarfa, C., Ludwig, A., Benham, A.L., Chen, Z., Patterson, D.M., Barbieri, E., Mestdagh, P., Sikorski, D.N. *et al.* (2011) A genome-wide search for promoters that respond to increased MYCN reveals both new oncogenic and tumor suppressor microRNAs associated with aggressive neuroblastoma. *Cancer Res.*, **71**, 3841–3851.
23. Forsythe, J.A., Jiang, B.H., Iyer, N.V., Agani, F., Leung, S.W., Koos, R.D. and Semenza, G.L. (1996) Activation of vascular endothelial growth factor gene transcription by hypoxia-inducible factor 1. *Mol. Cell Biol.*, **16**, 4604–4613.
24. Li, L.C., Okino, S.T., Zhao, H., Pookot, D., Place, R.F., Urakami, S., Enokida, H. and Dahiya, R. (2006) Small dsRNAs induce transcriptional activation in human cells. *Proc. Natl Acad. Sci. USA*, **103**, 17337–17342.
25. Huang, V., Place, R.F., Portnoy, V., Wang, J., Qi, Z., Jia, Z., Yu, A., Shuman, M., Yu, J. and Li, L.C. (2012) Upregulation of Cyclin B1 by miRNA and its implications in cancer. *Nucleic Acids Res.*, **40**, 1695–1707.
26. Dong, J., Kukula, A.K., Toyoshima, M. and Nakajima, M. (2000) Genomic organization and chromosome localization of the newly identified human heparanase gene. *Gene*, **253**, 171–178.
27. Jiang, P., Kumar, A., Parrillo, J.E., Dempsey, L.A., Platt, J.L., Prinz, R.A. and Xu, X. (2002) Cloning and characterization of the human heparanase-1 (HPR1) gene promoter: role of GA-binding protein and Sp1 in regulating HPR1 basal promoter activity. *J. Biol. Chem.*, **277**, 8989–8998.
28. Lu, W.C., Liu, Y.N., Kang, B.B. and Chen, J.H. (2003) Trans-activation of heparanase promoter by ETS transcription factors. *Oncogene*, **22**, 919–923.
29. Ogishima, T., Shiina, H., Breault, J.E., Tabatabai, L., Bassett, W. W., Enokida, H., Li, L.C., Kawakami, T., Urakami, S., Ribeiro-Filho, L.A. *et al.* (2005) Increased heparanase expression is caused by promoter hypomethylation and up-regulation of transcriptional factor early growth response-1 in human prostate cancer. *Clin. Cancer Res.*, **11**, 1028–1036.
30. Cohen, I., Pappo, O., Elkin, M., San, T., Bar-Shavit, R., Hazan, R., Peretz, T., Vlodavsky, I. and Abramovitch, R. (2006) Heparanase promotes growth, angiogenesis and survival of primary breast tumors. *Int. J. Cancer*, **118**, 1609–1617.
31. Baraz, L., Haupt, Y., Elkin, M., Peretz, T. and Vlodavsky, I. (2006) Tumor suppressor p53 regulates heparanase gene expression. *Oncogene*, **25**, 3939–3947.
32. Janowski, B.A., Younger, S.T., Hardy, D.B., Ram, R., Huffman, K.E. and Corey, D.R. (2007) Activating gene expression in mammalian cells with promoter-targeted duplex RNAs. *Nat. Chem. Biol.*, **3**, 166–173.
33. Nishi, K., Nishi, A., Nagasawa, T. and Ui-Tei, K. (2013) Human TNRC6A is an Argonaute-navigator protein for microRNA-mediated gene silencing in the nucleus. *RNA*, **19**, 17–35.
34. Peters, L. and Meister, G. (2007) Argonaute proteins: mediators of RNA silencing. *Mol. Cell*, **26**, 611–623.
35. Younger, S.T., Pertsemlidis, A. and Corey, D.R. (2009) Predicting potential miRNA target sites within gene promoters. *Bioorg. Med. Chem. Lett.*, **19**, 3791–3794.
36. Liao, J.Y., Ma, L.M., Guo, Y.H., Zhang, Y.C., Zhou, H., Shao, P., Chen, Y.Q. and Qu, L.H. (2010) Deep sequencing of human nuclear and cytoplasmic small RNAs reveals an unexpectedly complex subcellular distribution of miRNAs and tRNA 3′ trailers. *PLoS ONE*, **5**, e10563.
37. Majid, S., Dar, A.A., Saini, S., Yamamura, S., Hirata, H., Tanaka, Y., Deng, G. and Dahiya, R. (2010) MicroRNA-205–directed transcriptional activation of tumor suppressor genes in prostate cancer. *Cancer*, **116**, 5637–5649.
38. Cummins, J.M., He, Y., Leary, R.J., Pagliarini, R., Diaz, L.A., Sjoblom, T., Barad, O., Bentwich, Z., Szafranska, A.E., Labourier, E. *et al.* (2006) The colorectal microRNAome. *Proc. Natl Acad. Sci. USA*, **103**, 3687–3692.
39. Maes, O.C., An, J., Sarojini, H., Wu, H. and Wang, E. (2008) Changes in MicroRNA expression patterns in human fibroblasts after low-LET radiation. *J. Cell Biochem.*, **105**, 824–834.
40. Park, S.J., Cheon, E.J. and Kim, H.A. (2013) MicroRNA-558 regulates the expression of cyclooxygenase-2 and IL-1β-induced catabolic effects in human articular chondrocytes. *Osteoarthritis Cartilage*, **21**, 981–989.
41. Si, H., Sun, X., Chen, Y., Cao, Y., Chen, S., Wang, H. and Hu, C. (2013) Circulating microRNA-92a and microRNA-21 as novel

minimally invasive biomarkers for primary breast cancer. *J. Cancer Res. Clin. Oncol.*, **139**, 223–229.

42. Toscano-Garibay, J.D. and Aquino-Jarquin, G. (2014) Transcriptional regulation mechanism mediated by miRNA–DNA•DNA triplex structure stabilized by Argonaute. *Biochim. Biophys. Acta.*, **1839**, 1079–1083.
43. Zhang, H., Qi, M., Li, S., Qi, T., Mei, H., Huang, K., Zheng, L. and Tong, Q. (2012) MicroRNA-9 targets matrix metalloproteinase 14 to inhibit invasion, metastasis, and angiogenesis of neuroblastoma cells. *Mol. Cancer Ther.*, **11**, 1454–1466.
44. Zhang, H., Pu, J., Qi, T., Qi, M., Yang, C., Li, S., Huang, K., Zheng, L. and Tong, Q. (2014) MicroRNA-145 inhibits the growth, invasion, metastasis and angiogenesis of neuroblastoma cells through targeting hypoxia-inducible factor 2 alpha. *Oncogene*, **33**, 387–397.
45. Li, D., Mei, H., Qi, M., Yang, D., Zhao, X., Xiang, X., Pu, J., Huang, K., Zheng, L. and Tong, Q. (2013) FOXD3 is a novel tumor suppressor that affects growth, invasion, metastasis and angiogenesis of neuroblastoma. *Oncotarget*, **4**, 2021–2044.
46. Zheng, L., Pu, J., Qi, T., Qi, M., Li, D., Xiang, X., Huang, K. and Tong, Q. (2013) miRNA-145 targets v-ets erythroblastosis virus E26 oncogene homolog 1 to suppress the invasion, metastasis, and angiogenesis of gastric cancer cells. *Mol. Cancer Res.*, **11**, 182–193.
47. Zheng, L., Qi, T., Yang, D., Qi, M., Li, D., Xiang, X., Huang, K. and Tong, Q. (2013) microRNA-9 suppresses the proliferation, invasion and metastasis of gastric cancer cells through targeting cyclin D1 and Ets1. *PLoS ONE*, **8**, e55719.
48. Griffiths-Jones, S. (2004) The microRNA registry. *Nucleic Acids Res.*, **32**, D109–D111.
49. Zheng, L., Li, D., Xiang, X., Tong, L., Qi, M., Pu, J., Huang, K. and Tong, Q. (2013) Methyl jasmonate abolishes the migration, invasion and angiogenesis of gastric cancer cells through down-regulation of matrix metalloproteinase 14. *BMC Cancer*, **13**, 74.
50. Lin, C.W., Chang, Y.L., Chang, Y.C., Lin, J.C., Chen, C.C., Pan, S.H., Wu, C.T., Chen, H.Y., Yang, S.C., Hong, T.M. *et al.* (2013) MicroRNA-135b promotes lung cancer metastasis by regulating multiple targets in the Hippo pathway and LZTS1. *Nat. Commun.*, **4**, 1877.